Food & Function

ROYAL SOCIETY OF CHEMISTRY

PAPER

View Article Online
View Journal | View Issue

Cite this: *Food Funct.*, 2025, **16**, 2577

Characterization of different stages of Maillard reaction in soy: impact on physicochemical properties and immunogenicity of soy proteins†

Cresci-Anne Croes, *‡[a] Daniela Briceno Noriega,‡[a] Harry Wichers,[b] Huub F. J. Savelkoul,[a] Janneke Ruinemans-Koerts[a,c] and Malgorzata Teodorowicz[a]

The Maillard reaction (MR, glycation) frequently occurs during processing of soy-based products widely consumed in Western diets. MR leads to the formation of a number of chemically different structures called Maillard reaction products (MRPs), which include early glycation products and advanced glycation end products (AGEs). AGEs/MRPs were shown to modulate the immune response by interaction with specific receptors expressed on immune cells, such as the receptor for advanced glycation end products (RAGE). However, the structure–function relationship of MRPs formed during soy processing in relation to binding to AGE receptors has not been well studied. The aim of the present study is to characterize the MRPs formed during different heating times of soy proteins (SP) with glucose by analyzing the biochemical changes and to relate them to the functional changes, including binding to AGE receptors and stimulating immune cells. Our results demonstrated time-dependent differences in the biochemical characteristics of glycated SP compared with heated SP, which could be attributed to the different stages of MR and the diversity of MRPs. Moreover, the formation of AGEs over time was positively correlated with binding capacity to AGE receptors. Additionally, stimulating peripheral blood adherent monocytes with glycated SP resulted in increased gene expression levels of pro-inflammatory cytokines (IL-1β, IL-8 and TNF-α) when compared to non-glycated SP, suggesting that the formed AGEs bind to and activate receptors, such as RAGE. Our findings highlight the importance of studying immunomodulation upon processing of SP, which may lead to optimisation of the processing conditions of soy based food products.

Received 25th September 2024,
Accepted 8th February 2025

DOI: 10.1039/d4fo04400b

rsc.li/food-function

1. Introduction

In recent decades, soy proteins have been more frequently used in food products not only for their reported beneficial health effects, but also because they represent inexpensive and excellent sources of high-quality proteins.[1,2] However, since soy is rarely consumed raw, the majority of soy-based products contain highly processed soy proteins.[2] The production of these soy-based products usually involves thermal processing such as cooking and roasting, during which the Maillard reaction (MR, glycation) may occur.[3] The MR occurs between free amino groups of amino acids of proteins with the carbonyl group of a reducing sugar.[4–6] The MR always occurs during food processing or cooking, when proteins and reducing sugars are present together.[7] The speed of reaction and the type of formed products are highly dependent on physical variables, such as temperature and heating time, and on chemical ones such as pH, water activity, and type of sugar.[8] The chemistry of the MR is very complex encompassing a whole network of various reactions, with several stages which can be summarized as: (i) early phase with formation of Schiff bases, (ii) intermediate phase and formation of unstable Amadori products, and (iii) late reaction and formation of irreversible AGE products.[9,10] The term Maillard reaction products (MRPs) covers all early, intermediate and advanced products; hence, it encompasses a heterogeneous and complex group of compounds commonly found in heat-processed foods.[10–12] Higher temperatures together with prolonged heating results in the formation of Maillard reaction products (MRPs) typical of the later stages of the reaction.[8] Thus, the MR leads to chemical modifications of food proteins and hence the formation of new flavors, colors, aromas, making this reaction important from both the food industry and consumer perspective.[10,11]

[a]*Department Cell Biology and Immunology, Wageningen University and Research Centre, Wageningen, The Netherlands. E-mail: cresci_anne@hotmail.com*
[b]*Wageningen Food & Biobased Research, Wageningen University and Research Centre, The Netherlands*
[c]*Department of Clinical Chemistry and Hematology, Rijnstate Hospital, Arnhem, The Netherlands*

†Electronic supplementary information (ESI) available. See DOI: https://doi.org/10.1039/d4fo04400b

‡These authors have contributed equally to this work and share first authorship.

It is clear that MR alters the structure of food proteins, also influencing their digestibility, nutritional value *via* lysine blockages, but also some of the functional properties like immunomodulatory properties of specific proteins.[1,4,5] While endogenous MRPs have been linked to the pathogenesis of a number of diseases, such as diabetes, neurodegenerative diseases and cardiovascular diseases, the role of food-derived MRPs in the development of those diseases is still under debate.[12] Some MRPs that can be formed during food processing are N^{ε}-(carboxymethyl)lysine (CML) and N^{ε}-(carboxyethyl) lysine (CEL).[13,14] Additionally, some AGEs have been shown to interact directly with immune cells *via* specific receptors, including receptor for advanced glycation end products (RAGE), CD36, a member of the class B scavenger receptor family, and Galectin-3, and these interactions may induce oxidative stress and activate inflammatory cascades.[1,5,9,10] For example, it has been reported that CML promotes macrophage lipid uptake *via* CD36 and RAGE, which may lead to the formation of foam cells.[14] This suggests that dietary MRPs/AGEs may add to the pool of endogenous AGEs and promote pathological complications of common non-communicable diseases, such as cardiovascular diseases and diabetes.[13–18] Moreover, activation of the RAGE receptor expressed on the surface of various immune cells[9] leads to activation of pro-inflammatory responses *via* transcription factor NFkB,[9,19–22] contributing to a number of metabolic diseases. While it has been shown that accumulation of endogenous AGEs leads to such inflammatory consequences,[23,24] the data regarding consequence of dietary AGEs are mixed. In mice, dietary supplementation with AGE CML caused elevated serum levels of CML as well as insulin resistance, impacting cardiac function by altering myocardial glucose metabolism and promoting myocardial remodeling.[13] However, a human study by Linkens *et al.* did not find an association between dietary AGEs and negative health outcomes[25] but higher habitual intake of dietary AGEs led to higher plasma dicarbonyl concentration and skin AGEs in humans,[26] suggesting the possibility of dietary AGEs to interact with immune cells. Such an activation of immune cells *via* RAGE was reported by *in vitro* studies using various AGE-modified food proteins.[27,28] However, it is not clear yet which AGE structures are responsible for RAGE activation as well as if RAGE activation can be regulated by controlling the conditions of MR in food systems.

Since soy proteins are frequently used in food industry and at the same time it is known that soy proteins are very potent for glycation,[2] it is important to study the consequences of glycation on the bio-functional properties of soy proteins. Although very detailed studies and review were published describing the different aspects of the kinetics of the MR,[8,29,30] the bio-functional activity of MRPs formed at different conditions was not included as a read-out system. Therefore, the goal of this study was to provide new insights into the role of dietary soy-derived MRPs, formed at different stages of the reaction, in inducing an immune response. More precisely, we aimed to characterize the MRPs formed during different heating times of soy proteins with glucose by analysing their biochemical changes and evaluating their immune-modulatory effects, such as binding to AGE receptors and stimulating immune cells to secrete pro-inflammatory cytokines.

2. Materials and methods

2.1. Soy protein extracts (SPEs)

The protein extraction from soy flour (SPEs) was performed according to L'Hocine *et al.*,[31] with some minor modifications. The precipitation pH was adjusted to 9.0, the washing of the precipitate was done with deionized water (Milli Q, MQ, Millipore, St Louis, MO, USA) and performed once instead of twice to improve protein recovery.[31] The starting material was 5 grams of soy flour (Sigma Aldrich, St Louis, MO, USA, S9633), which contains 2.2 grams of protein, according to the manufacturer. The flour was dissolved in water at 55 °C at a ratio of 1 : 10 (w/v). The supernatant was separated from the insoluble part by centrifugation (30 minutes, 9000*g* at 4 °C), and the pellet was collected to perform the re-extraction. The pellet was stirred for 2 h at room temperature (RT) and then centrifuged at 9000*g* for 20 minutes at 4 °C. The obtained precipitate was washed twice and spun down. The pH of the protein extract was measured and adjusted to 7.5 with 2 M NaOH, and the protein concentration was determined by absorbance at 280 nm using NanoDrop. The SPEs obtained consisted of 44.2% dispersible protein and were estimated to be 14.2 mg ml^{-1}.

After extraction, the SPE was dissolved in PBS and distributed in Eppendorf tubes. Glucose was added in a ratio 1 : 2 (w/w, protein/glucose), and same volume of PBS was added to the control. All samples were heated at 100 °C for 5, 10, 20, 30, 45, 60, 90 and 120 minutes with and without glucose, in a heating block. A non-heated control was included as the reference point. After heating, the samples were cooled on ice and stored at −20 °C.

2.2. Sodium dodecyl sulphate-polyacrylamide gel electrophoresis (SDS-PAGE)

Soy protein extracts were separated by SDS-PAGE under reducing conditions using Bio-Rad equipment. Proteins were loaded at a concentration of 20 μg per well on a 12.5% polyacrylamide gel. After protein separation, the gel was stained using GelCode Blue Stain Reagent (Thermo Scientific). A molecular weight marker (Precision Plus Protein Dual Color standards, Bio-Rad) was included.

2.3. Structural properties of soy proteins

2.3.1. O-phthaldialdehyde (OPA) assay. The assay was performed as described previously by Nielsen *et al.*[32] The proteins were diluted to the concentration of 2 mg ml^{-1}. Appropriate blanks were prepared. Samples were distributed at a volume of 30 μl per well into 96-well plate. L-Leucine (2.5–0.078 mM) was selected for the standard curve because it was identified as one of the amino acids with optimal reactivity with OPA according to Nielsen *et al.* To each well, 200 μl of a freshly pre-

pared reagent of sodium tetraborate (0.10 M), SDS (3.5 mM), OPA (6.0 mM) and dithiothreitol (5.7 mM) was added. The plate was incubated at RT for 20 minutes, after which the absorbance was measured at 340 nm. The amount of free amino groups was calculated from the standard curve obtained for L-leucine (normally linear for these concentrations).

2.3.2. UV-Vis. Intermediate MRPs were detected by recording the UV-absorbance at 294 nm to measure intermediate products of the MR, 420 nm to measure the advanced products of the MR. The results of the protein samples were corrected with the blank. The proteins were diluted to 2 mg ml^{-1} and pipetted onto a clear 96-well plate. A PBS blank was added.

2.3.3. Fluorescence and fructosamine assays. The maximum excitation and emission were determined previously (excitation at 340 nm, emission at 435 nm), and fluorescence was recorded to detect advanced MRPs. The samples at a concentration of 2 mg ml^{-1} were pipetted into a white, non-transparent plate. The maximum excitation of the samples was tested between 320 and 380 nm with the emission wavelength at 425 nm. The maximum emission was tested from 380 to 480 nm in steps of 10 nm. Finally, the fluorescence was measured at the optimal excitation and emission wavelength.

A fructosamine commercial kit (Kamiya Biomedical Company, Seattle, WA, US) was used. The methods were adapted for a 96-well plate, as this kit was not designed for small-scale use; thus, the volumes used were 4 times lower than in the original protocol. The samples were diluted to 2 mg ml^{-1} and pipetted into 96-well plate in a volume of 12.5 μl. Then, 250 μl reagent was added and the plate was incubated for 10 minutes at 37 °C. The absorbance was measured at 535 nm. The plate was incubated for another 5 minutes at 37 °C and the absorbance was measured again at 535 nm. The concentration of fructosamine was then calculated using the following formula, where A_1 is the absorbance from the first measurement and A_2 is the absorbance from the second:

$$\frac{A_2\,\text{sample} - A_1\,\text{sample}}{A_2\,\text{calibrator} - A_1\text{calibrator}} \times \text{conc. of calibrator} = \text{conc. fructosamine in sample}$$

2.3.4. Quantification of MRPs. uHPLC-ESI-MS/MS was used to measure the quantities of furosine, N^{ϵ}-carboxymethyl lysine (CML), and carboxyethyl lysine (CEL) as described by Zenker *et al.*[33] To ensure accuracy, Solid Phase Extraction (SPE) recovery checks were conducted on samples, including three quality controls. Each sample, set to a concentration of 6 mg ml^{-1}, underwent heating with 1 ml 6 M HCl at 110 °C in glass heating tubes for 22 hours. Next, 400 μl of the resulting solution was transferred to an MS vial and dried in a vacuum concentrator (SpeedVac, Thermo Fisher Scientific, Waltham, Massachusetts, USA) then reconstituted in a mixture of 500 μl acetonitrile and MilliQ water (1 : 1 v/v). Subsequently, the solution was spiked with furosine-d4, CML-d4, and CEL-d4, bringing the final concentration to 500 ng ml^{-1}. The analysis was conducted using a Kinetex 2.6 μ HILIC 100A, 100 × 2.1 mm column (Phenomenex, Torrance, California, USA) at a temperature of 35 °C. The elution process involved ultrapure water with 0.1% formic acid (eluent A), acetonitrile with 0.1% formic acid (eluent B), and 50 mM ammonium formate (eluent C). The flow rate was maintained at 0.4 mL min^{-1} following the gradient: (0/80/10), (0.8/80/10), (3.5/40/10), (6.5/80/10), (8.0/80/10), (11/80/10). Ionization was set to a positive mode, with a spray voltage of 3500 V, vaporizing temperature of 250 °C, and sheath gas pressure of 60 psig. The capillary temperature was regulated at 290 °C.

2.3.5. Browning. The browning of the samples, which measures the advanced stage of the MR, was determined based on methods described by Buera & Resnik *et al.*[34,35] The proteins were diluted to 2 mg ml^{-1} and pipetted in triplicate onto a clear 96-well plate. The absorbance was measured at 625, 495, 445, and 550 nm. This value was then corrected and converted to the transmission ($10^{-A} = T$). The transmission values were then used to calculate X ($X = T_{625} \times 0.42 + T_{550} \times 0.35 + T_{445} \times 0.21$), Y ($Y = T_{625} \times 0.2 + T_{550} \times 0.63 + T_{495} \times 0.17$) and Z ($Z = T_{495} \times 0.24 + T_{445} \times 0.94$). The browning index (Br) was then calculated as follows:

$$\text{Br} = x - \frac{0.31}{0.172} \times 100$$

where $x = X/(X + Y + Z)$

2.4. Functional properties of soy proteins

2.4.1. Antioxidant assay (DPPH). The method was adapted from Gu *et al.*[36] In short, samples were diluted to 2 mg ml^{-1} for analysis. Additionally, a blank of PBS along with the positive control of Trolox were prepared. The samples were plated in six-fold (125 μl per well). Subsequently, methanol was added to half of the samples and to the other half DPPH dissolved in methanol (0.2 mM) was added. The contents of each well were mixed and the plate was incubated in the dark at room temperature (RT) for 30 minutes. After this, the absorption was measured at 535 nm and the radical scavenging activity (RSA) was calculated using the formula:

$$\text{RSA} = \left[1 - \frac{A_{\text{sample}} - A_{\text{control}}}{A_{\text{blank}}}\right] \times 100$$

2.4.2. AGEs receptor inhibition ELISA binding assay. This assay was performed as described by Zenker *et al.*[33] to determine the binding affinity of sRAGE. The coating material consisted of glycated SPEs with glucose (heated for 90 min at 100 °C under wet conditions). Transparent high binding ELISA plates (Greiner Bio-One, Kremsmuenster, Austria) were coated with the SPE glycated for 90 minutes (G90) and incubated for 12 h at 4 °C. The sample protein concentration was adjusted to 25 μg mL^{-1} using a solution containing 1.5% bovine serum albumin (BSA), 0.025% tween, and 10 mM PBS (PBST), with the optimal protein concentration determined from a pre-experiment. Before being added to the ELISA plate, the samples were pre-incubated with 1 μg mL^{-1} sRAGE in a ratio 1 : 1 (*v*/*v*) ratio for 45 min at 37 °C on a Nunc™ polystyrene plate (Thermo Fisher Scientific, MA, USA). The coated ELISA plate was then blocked with 3% BSA in PBS (*w*/*v*) for 1 h at

room temperature and washed with PBST (washing was repeated after each step of the ELISA). After blocking, the pre-incubated sRAGE/sample mixture was transferred to the ELISA plate and incubated for 1 h at 37 °C. After washing, the anti-sRAGE antibody was added at a concentration of 0.25 μg mL^{-1}, and the plate was incubated with shaking for 30 min at room temperature. After washing, an anti-mouse polyclonal goat HRP-conjugated antibody was added at a concentration 0.25 μg mL^{-1}, and the incubation was continued for 30 min at room temperature. The signal was detected with TMB. The color reaction was measured at 450 nm, with a 620–650 nm reference, using a Filter Max F5 multi-mode microplate reader (Molecular Devices, San Jose, CA, USA). Each sample was measured in triplicate. Amyloid-β was used as a positive control, while ovalbumin was used as a negative control. Inhibition was calculated using the formula below, where Abs_{Max} is the absorbance obtained from sRAGE without a competition agent, Abs_{Min} is the absorbance obtained from sRAGE without a competitive agent, and Abs_{sample} is the absorbance obtained from the mixture of sRAGE and each sample. High inhibition indicates high sRAGE binding affinity.

$$\text{Inhibition}\,[\%] = \left[\frac{\text{Abs}_{\max} - (\text{Abs}_{\text{sample}} - \text{Abs}_{\text{Min}})}{\text{Abs}_{\text{Max}} \times 100}\right]$$

2.4.3. Primary adherent monocytes stimulation and Cytokine measurement. Blood samples were collected from five healthy adult donors in EDTA tubes. Peripheral blood mononuclear cells (PBMCs) were isolated according to previously described protocols.[37] After the second wash, PBMCs were resuspended in 1 ml of RPMI 1640-Glutamax medium, supplemented with 10% FBS, 1% MEM non-essential amino acids, 1% Na-Pyruvate and 1% Pen/Strep, and then counted before further monocyte isolation. Monocytes were isolated by using EasySep Human Monocyte Isolation kit (Stem cell technologies, #19359), then seeded at 1×10^6 cells per 2 ml per well on a 24-well plate and allowed to rest for 2 hours before stimulation, resulting in adhesive PBMC-derived monocytes. The adhesive PBMC-derived monocytes were stimulated with glycated soy at 25 μg ml^{-1} for 3 hours. RNA was isolated using the RNeasy mini kit (Qiagen). For harvesting, cells were washed with PBS, then RLT buffer containing 1% β-mercaptoethanol was added directly to the wells. The sample was then passed through a needle attached to a 1 mL syringe. To the homogenized lysate, 350 μl of 70% ethanol was added, bringing the total volume to 700 μl, which was added to the RNeasy Mini column and centrifuged for 30 seconds at 10 000 rpm. After washing, 80 μl of DNase solution was added to the column and incubated for 15 min at room temperature. The column was washed twice with buffer and eluted with 30 μl of RNase-free water. RNA concentration was measured on the NanoDrop spectrophotometer. cDNA was synthesized from 250–500 ng of RNA per samples using the SuperScript III kit (Invitrogen), following the manufacturer's instructions, with a T-professional PCR instrument (Westburg, Leusden, Netherlands). For qPCR analysis, each tube contained 1× SYBR Green master mix, 3 μM of forward and reverse primers, and 1 μg of cDNA. Samples were run on a Qiagen Rotor-Gene Q 5plex HRM device (Qiagen, Hilden, Germany). The primers are listed in ESI Fig. 2.† Gene expression was calculated from data retrieved from *via* Rotor-Gene Q software (Qiagen) and converted to fold change using the Pfaffl method. Expression is normalized to the PUM1 gene. GraphPad Prism 9.5.1. (Boston, MA, USA) and Student's *t*-test were used for statistical analysis. In a pilot experiment to block RAGE, the RAGE antagonist FPS-ZM1 was used at a concentration of 13 μM, and primary adherent monocytes were treated with 250 μg ml^{-1} of G-SP for 24 hours. RNA isolation, cDNA synthesis, and qPCR measurements were performed as described above.

2.4.4. Western blot analysis of p-NFkB p65. Differentiated THP-1 or adherent primary monocytes were treated with 25 μg ml^{-1} of glycated soy for 10 minutes, followed by whole-cell lysis. Cells were lysed using commercial RIPA buffer supplemented with 1× protease/phosphatase inhibitor (Cell Signaling, Massachusetts, United States), followed by measurement of concentration using the NanoDrop. Whole-cell lysate was then prepared for SDS gel electrophoresis as described previously. Subsequently, the gel, membrane, and blot paper were equilibrated in Western Blot Semi-Dry Blot Buffer for 30 min and stacked inside of a trans-Blot SD Semi-Dry Transfer Cell and run at 15 V for 35 min. Next, the membrane was washed twice with TBS-T, followed by blocking with 5% milk in TBS-T for 2 h at 4 °C. The membrane was then washed 3×, followed by incubation with primary antibody (Phospho-NF-κB p65 (Ser536) (93H1) Rabbit mAb, Cell Signaling) overnight at 4 °C. Next, the membrane was washed 3× in TBS-T, followed by incubation with detection antibody for 1 h at room temperature. Finally, the membrane is washed 3× in TBS-T, followed by detection by means of ECL with a BioRad Chemidoc. Protein expression was quantified using the ImageLab software. Protein expression was normalized to β-Actin Antibody (Cell Signaling, #4967).

2.5. Statistical analysis

Statistical analysis was conducted using GraphPad Prism version 9.5.1. A one-way ANOVA was employed for comparing multiple samples, while a Student's *t*-test was used for pairwise comparisons. A *p*-value of less than 0.05 was considered to indicate statistical significance ($p < 0.05$).

3. Results

3.1. Heat processing of soy profoundly alters its structure, and in the presence of glucose leads to aggregates

The extent and types of MR formed during different heating times at 100 °C were assessed by various methods. As some pellet formation occurred, leading to a decreased protein concentration during these procedures, we focussed on analysing the soluble components only.

To study how glycation over time affected the protein structures of heated soy protein (H-SP) and glycated soy protein (G-SP), SDS-PAGE was performed (Fig. 1A and B). The

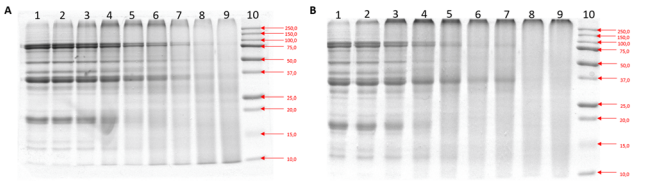

Fig. 1 SDS PAGE results depicting separation by molecular weight of (A) Heated Soy Proteins (H-SP), (B) Glycated Soy Proteins (G-SP).

SDS-PAGE separation of the raw soy protein extract showed the characteristic bands of the major soy proteins, β-conglycinin (α′, α, and β) and glycinin (As and Bs) subunits (ESI Fig. 3†). As heating time increased, the intensity of the characteristic protein bands decreased, and more intense bands of high molecular weight in the upper part of the gel were observed. The G-SP showed slightly more reduction in band intensity compared to the H-SP (Fig. 1A and B). Additionally, the smeared zones at the top became darker after 10 min of heating, particularly for the G-SP, suggesting that glycation promotes the formation of aggregates with higher molecular weight. Thus, the results of the SDS-PAGE show that heating and glycation affect the structure of SPEs.

3.2. Analysis of glycated soy proteins reveals early, intermediate and advanced phases of Maillard reaction

To further measure characteristic and structural changes in soy protein during MR, we analyzed H-SP and G-SP *via* the OPA-assay, UV-vis, fructosamine, fluorescence, browning, the DPPH assay, and UPLC-MS/MS.

The OPA assay measured the amount of free amino groups, which are major reactants of the MR, in both H-SP and G-SP. The results showed a sharp decrease within the first 20 minutes, reaching a maximum after 60 minutes of glycation being at the level of 0.77 (Fig. 2A). Thus, a significant reduction in free amino groups was observed at 60, 90 and 120 minutes of treatment during glycation with glucose.

To measure the formation of intermediate and late MRPs in a non-specific manner, UV-Vis was used at wavelengths of 294 nm (intermediate MRPs) and 420 nm (advanced MRPs), respectively. The UV-Vis results showed that absorbance at 294 nm for the G-SP increased linearly with time, reaching a plateau after 90 minutes, with an absorption level 5 times higher than that of H-SP (Fig. 2B). A similar linear increase was observed for G-SP at 420 nm, reaching a maximum after 120 minutes, which was 7 times higher than that of H-SP (Fig. 2C).

To continue characterization of the type of MRPs formed at different time points of heating of SPE, fructosamine, an early MRP and important AGE precursor, was measured.[38,39] The results showed that the concentration of fructosamine in H-SP was constant and did not exceed of 0.3 mM, whereas in G-SP, a linear increase in fructosamine concentration was observed immediately after heating, reaching a plateau after 45 minutes (>1.5 mM) (Fig. 2D). These results, together with OPA results,

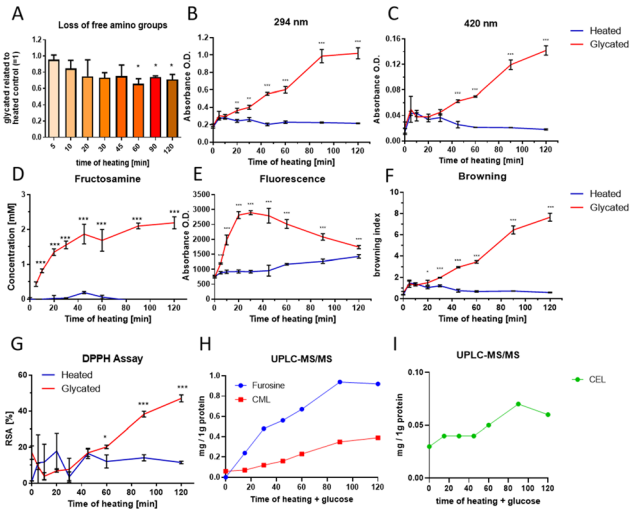

Fig. 2 Structural changes of heat treated and glycated of soy proteins. Results of the Structural Properties of heated and glycated soy proteins *vs.* glycated soy in a heating time series: (A) OPA assay depicting loss of free amino groups as a result of glycation. Data shown is ratio relative to heat soy control, (B) UV-vis at 294 nm depicting structural change of the glycated soy protein *vs.* heated soy protein, (C) UV-vis at 420 nm depicting structural change of the glycated soy protein *vs.* heated soy protein, (D) fructosamine assay depicting fructosamine detection in glycated soy *vs.* heated soy, (E) fluorescence assay depicting the detection of fluorescence AGEs in glycated soy *vs.* heated soy, and (F) browning assay depicting formation of MRP-related browning in glycated soy *vs.* heated soy. (G) Radical Scavenging Activity (RSA) of the samples *via* DPPH assay, (H) detection of CML and furosine, and (I) CEL *via* UPLC-MS/MS. Students *T*-test was used to determine significance of glycated soy *vs.* heated soy, where * = $P < 0.05$, ** = $P < 0.01$, *** = $P < 0.001$.

indicate that the early-stage formation of the MR started after 5 minutes of heating. To assess the formation of fluorescent AGEs in SPE-glycation, fluorescence in the G-SP samples was immediately observed to increase and then increased significantly further after 5 minutes, reaching a maximum after 30 minutes. This final fluorescence level was 3-times higher for G-SP compared to H-SP (Fig. 2E). Additionally, CML, furosine and CEL were measured in G-SP *via* UPLC-MS/MS. A dose–response increase was noted for both CML and furosine in G-SP with increased glycation time, with furosine plateauing at 90 minutes, while CML Levels continued to increase at a steady rate (Fig. 2H). CEL increased after 10 minutes of soy glycation, followed by a steep dose–response increase in CEL formation from 40 minutes to 90 minutes of glycation (Fig. 2I).

Next, we measured the browning index of treated soy protein and the antioxidant capacity of treated extracts. The browning index is often used as a predictor of melanoidin formation, the final brown products of the MR,[39,40] and melanoidins are known for their antioxidant capacity.[5] The browning of the H-SP was stable and did not exceed a browning index value of 1.5, while the browning of the G-SP showed a linear increase with time, and after 120 minutes, its value was 13.6 times higher than that of the H-SP at the same time (Fig. 2F). To measure the antioxidant capacity of the extracts, a DPPH assay was performed. By conducting the DPPH assay, it is poss-

ible to measure from which timepoint in the MR the antioxidant properties begins, which can be correlated to other advanced MR readouts such as browning, likely showing presence of melanoidins. A significant increase in RSA antioxidant capacity was observed from 60 minutes for G-SP, with a steady increase up to 120 minutes, which indeed correlated with the increasing browning index at the same time points (Fig. 2G).

In summary, the results show that the formation of intermediate MRPs starts after the first minutes of heating, as shown by the UV-vis assay, with the fructosamine, furosine, CEL, and fluorescence results pointing toward the formation of mainly early MRPs in the first 30 minutes. Moreover, formation of intermediate MRPs started after ~30 minutes of heating, with a rapid rise in CEL and reaching a plateau after 90 minutes of heating, as shown by the CEL and UV-vis at 294 nm. Lastly, 420 nm readings, browning, and CML showed a steady increase, reaching their highest peak at 120 minutes, highlighting the advanced phase. These results show that the types of MRPs and AGEs obtained in SPE – glycation strongly depend on the applied heating time.

3.3. Glycation of soy protein at 100 °C increases its binding affinity to AGE receptors

To measure the impact of soy glycation on receptor binding, an inhibition ELISA assay against sRAGE was optimized (ESI Fig. 4†). Fig. 3A shows the effect of different concentrations of G-SP heated at different timepoints on the binding to RAGE receptor. Dose–response curves were observed for all concentrations of G-SP tested, with longer heating times showing the highest inhibition and thus strongest binding to sRAGE (Fig. 3A). Specifically, a sharp rise in inhibition was observed between 2.5 μg ml^{-1} and 25 μg ml^{-1} for all G-SP samples, with G-SP at 90 and 120 minutes showing the steepest increase (Fig. 3A). A positive correlation between RAGE binding and heating time for G-SP was found (R^2 = 0.9456), but not for H-SP (R^2 = 0.5135) (Fig. 3B), suggesting a direct interaction between RAGE and MRPs/AGEs, rather than with heated protein.

Based on the results from Fig. 3A, G-SP at 25 μg ml^{-1} was chosen to study the binding to RAGE, as well as to CD36 and Galectin-3 receptors, over time. A dose–response curve was observed for RAGE and CD36. However, for Galectin-3, a steady increase was observed up to 60 minutes, followed by a sharp decline (Fig. 3C). To correlate receptor binding patterns with the levels of defined MRPs in the samples, a correlation analysis was performed. A positive correlation was observed between CML levels in the samples and binding to RAGE (R^2 = 0.9698) and CD36 (R^2 = 0.9573); CEL levels in the samples and binding to RAGE (R^2 = 0.7507) and CD36 (R^2 = 0.7936); and furosine content and binding to RAGE (R^2 = 0.9398) and CD36 (R^2 = 0.9322) (Fig. 3D). These results indicate specific interactions between MRP structures at different stages of formation and selective receptors expressed on immune cells. ESI Fig. 5† shows the ratios of AGE receptors and several other parameters measured in this study, revealing further that RAGE ratios are higher at later stages, galectin-3 binding skews towards early/intermediate, while CML formation skews towards later stages.

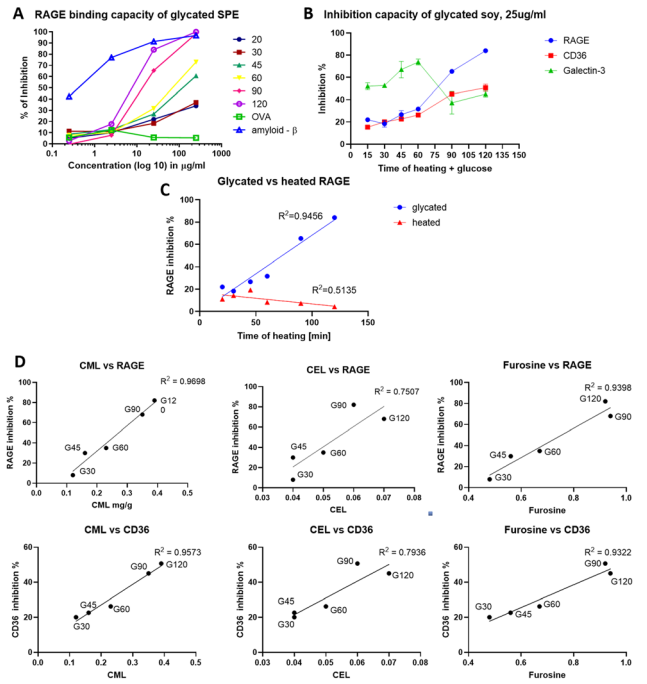

Fig. 3 Results of the Functional Properties of heated and glycated soy proteins assays in regard to receptor binding. (A) RAGE binding capacity of G-SP at different concentrations; (B) inhibition capacity of G-SPs for RAGE, Galectin-3 and CD36 at a concentration of 25 μg ml^{-1}; (C) correlation between time of heating and capability to inhibit sRAGE. (D) Correlation between MRPs and inhibition capacity of G-SP to receptors. OVA as the negative control and amyloid–β as the positive control.

3.4. Stimulation of macrophages with glycated soy causes an increase in pro-inflammatory markers

To investigate the immunomodulatory responses of advanced glycated soy proteins, we stimulated PBMC-derived adherent monocytes from 5 donors with G-SP and H-SP (heated for 90 min) for 24 hours, followed by gene expression analysis of inflammatory markers *via* qPCR (Fig. 4). Comparison of cytokine expression among the different donors in response to H-SP and G-SP showed consistently higher transcription levels of all investigated cytokines (IL-1β, IL-8, TNFα, and IL-10) in the G-SP samples compared to H-SP, although variation between donors was observed (Fig. 4A). When analyzing the gene expression profile of receptors, some donors individually showed an increased tendency in RAGE, Galectin-3, CD86, and DC-SIGN in response to G-SP treatment. However, when combining the response profiles of all donors tested, only CD209 expression was significantly upregulated at the transcript level (Fig. 4B).

To learn more about the immunogenic properties of glycated soy, we decided to perform a follow-up pilot experiment to explore the phosphorylation of NF-kB p65 in macrophages in response to stimulation with G-SP heated for 90 minutes. THP-1 differentiated macrophages and primary-derived adherent monocytes from one donor were both treated with G-SP for 10 minutes, followed by western blot analysis. Stimulation

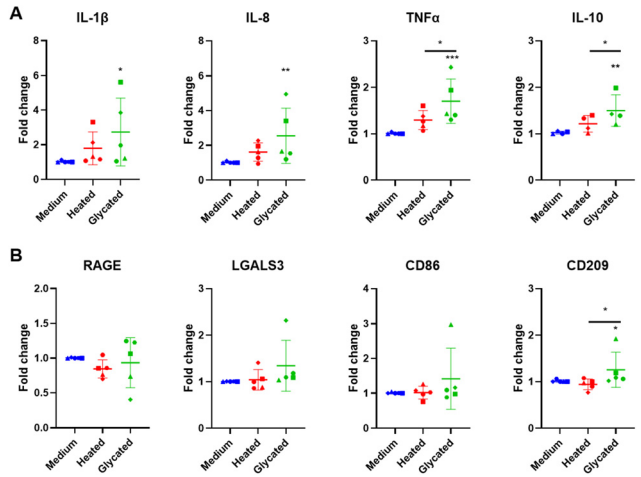

Fig. 4 Cytokine gene expression from PBMC-derived adherent monocytes by peripheral blood mononuclear cells (PMBCs) derived from blood of 5 healthy donors after stimulation with H-SP and G-SP 90 min for 24 hours. (A). gene expression of cytokines, (B) gene expression of receptors. Data shown is duplicate samples from 5 healthy donors. Students *T*-test was used to determine significance of glycated soy *vs.* medium if no line indicated, where * = $P < 0.05$, ** = $P < 0.01$, *** = $P < 0.001$.

with glycated soy led to an increased expression of p-NF-kB p65 in both THP-1 cells and adherent monocytes from the donor, although this increase was not significant (Fig. 5).

Lastly, we conducted a pilot experiment in primary adherent monocytes from one donor, using the RAGE antagonist FPS-ZM1 to investigate the impact of blocking RAGE on the G-SP inflammatory response. We found that FPS-ZM1 strongly

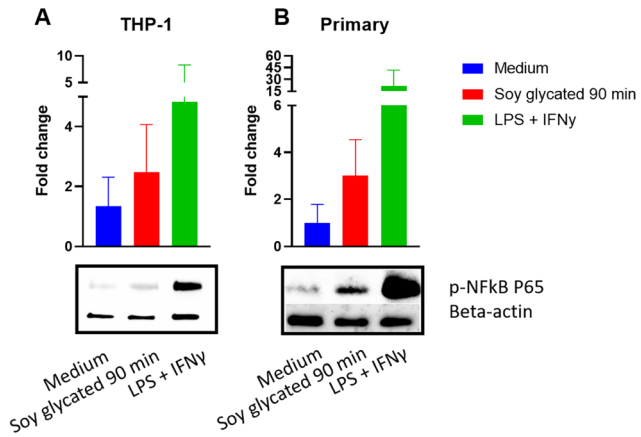

Fig. 5 Expression of phosphorylated NFkB p65 shows an increased trend in macrophages after stimulation with glycated soy. Expression of phosphorylated NFkB P65, analyzed by western blot (A) THP-1 differentiated into macrophages, stimulated with 25 μg ml^{-1} glycated soy or 100 ng ml^{-1} LPS and 10 ng ml^{-1} IFNγ for 10 minutes, data is representative of 3 replicates. (B) Primary derived adherent monocytes from one donor, stimulated with 25 μg ml^{-1} glycated soy or 100 ng ml^{-1} LPS and 10 ng ml^{-1} IFNγ, data is representative of two replicates. Quantified data based on the adjusted volume normalized to beta actin. Data was processed and quantified using the ImageLab software from BioRad.

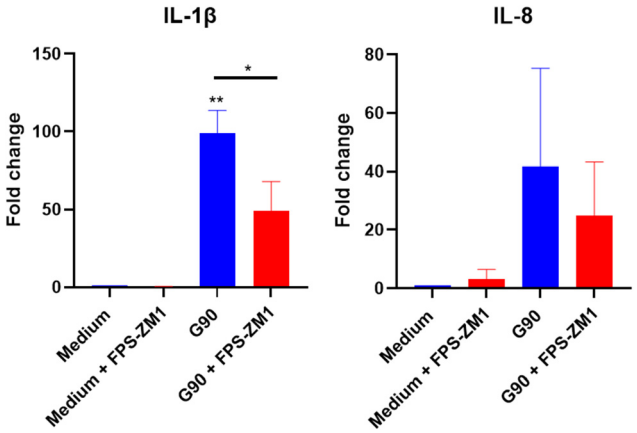

Fig. 6 Gene expression of cytokines after applying a RAGE antagonist to block G-SP induced inflammatory response in primary adherent monocytes. Primary adherent monocytes were pre-heated with 13 μM of FPS-ZM1 for 1 hour before stimulation with 250 μg ml^{-1} G-SP 90 min for 24 hours, followed by RNA isolation, cDNA synthesis, and qPCR analysis. Data shown is from biological replicate of one donor. Significance determined *via* one-way ANOVA analysis.

decreased the G-SP induced IL-1B and IL-8 response (Fig. 6). It is important to note that a higher concentration of G-SP was used in this experiment, namely 250 μg ml^{-1}, explaining the higher inflammatory responses compared to Fig. 4 and highlighting that higher concentrations of G-SP lead to increased immunogenicity.

4. Discussion

In this study we evaluated eight different time/temperature combinations for the glycation of soy proteins with glucose, by examining the impact on their structural and physiological properties. The effects of the MR were analyzed both at the kinetic and the functional levels. The present study revealed time-dependent differences in the characteristics and functional properties of glycated soy *versus* heated soy, which are linked to the various stages of the MR. While we described the following paragraph in stages, it must be noted that a number of MRPs are formed concurrently across multiple stages of MR making the complete separation of the stages and their individual analysis difficult to assess precisely. Therefore it is more accurate to consider the advantage of one of the stages over the others. Ratios calculated form our dataset, helped to set the segmentation of the different stages. As such, based on the AGE receptor binding and induced CML ratios *vs.* our measured parameters, we can delineate that early stages dominate between 0–30 minutes, intermediate between 30–90 minutes, and advanced/late stages from 90 minutes onwards.

4.1. Early MR stages

At the early stages of the MR, we observed increased formation of early MRPs (fructosamine and furosine). Moreover, we observed a significant loss of free amino groups, corroborating

earlier findings.[41–43] Interestingly, the reduction in free amino groups appeared to stabilize after 20–30 minutes, suggesting that the early phase of the MR occurs within this time window. This conclusion is further supported by the rapid increase in fructosamine and furosine, both early MRPs, within the first 30 minutes. Fluorescent MRPs, which are often linked to the formation of browning pigments, also increased rapidly in the early stages. This aligns with previous reports indicating that fluorescent MRPs, such as pentosidine,[4,5] can serve as precursors to browning.[42,44] It was previously reported that during the digestive process in meal-resembling systems, high fructosamine levels correlated with further formation of cross-linked fluorescent adducts, like pentosidine.[38] Pentosidine, although not-specifically measured, is likely produced as a result of glucose glycation of soy protein.[45] Notably, the SDS-PAGE analysis showed that heating soy protein, both with and without glucose, significantly altered the migration pattern of proteins in the gel. This effect was more pronounced in the glycated soy protein, which formed more aggregates as early as 10 minutes. Crosslinking AGEs, such as pentosidine,[45–47] likely contributes to aggregation in our samples. Markedly, the fluorescence in G-SP samples significantly increased during the early stage, but began to sharply decrease after approximately 40 minutes, suggesting formation of non-fluorescent advanced reaction products.[46] This observation supports previous studies reporting a peak in fluorescence intensity followed by a gradual decline.[48–51] The increase in early MRPs also correlated with increasing levels of RAGE, CD36 and Galectin-3 binding, although this binding was consistently below 30% of inhibition. Our receptor binding data are in line with previous studies revealing that early MRPs present in glucose glycation of albumin also bind to RAGE.[52] Remarkably, the binding of G-SP to Galectin-3 at the early stage was about three times higher compared to binding to RAGE and CD36 at this stage. Our receptor binding data are in line with previous studies revealing that early MRPs present in glucose glycation of albumin also bind to RAGE.[52,53] Moreover, aggregates were also shown to be recognised by RAGE, CD36 and Galectin-3, which could potentially explain the observed binding to those receptors.[54] Lastly, the endogenous modification of proteins with the fluorescent compound pentosidine has been reported to be linked with inflammation, chronic kidney disease and cardiovascular diseases.[47] However, the effect of dietary pentosidine on inflammatory processes is not yet clear.[55]

4.2. Intermediate MR Stages

We propose that intermediate stage of the MR in our system dominate after 30 minutes of heating until around 90 minutes. This conclusion is based on UV-vis measurements at 294 nm, which detect intermediate MRPs.[48] These measurements indicated the highest peaks between 60 and 90 minutes, consistent with the degradation of Amadori products and the formation of more stable MRPs.[39,49,50] This time interval is also characterized by a sharp increase in furosine, CML and CEL, though the relative amount of CEL produced was small compared to Furosine and CML. Notably, a strong linear correlation was found between CML and Furosine, indicating that furosine increases as glucose-derived AGEs are formed. The formation of intermediate MRPs leads to a strong increase in RAGE binding between 60 and 90 minutes. Interestingly, the level of fluorescent AGEs decreased in G-SPs heated longer than 45 minutes, indicating that non-fluorescent AGEs may be primarily responsible for receptor binding in later stages. Notably, a rapid decrease in Galectin-3 binding was observed, which correlates with the strong decrease in fluorescent AGEs. This could indicate a relationship between fluorescent MRPs and Galectin-3 binding. This is a novel finding, indicating that Galectin-3 may preferentially bind to fluorescent AGEs like pentosidine[45] in the early/intermediate stages. As for CD36, only a steady increase was noted in the intermediate stage. Although it is known that Galactin-3 receptor can bind AGEs there are no studies analysing the kinetics of such a binding for the different stages of MR and the different types of MRPs. Therefore the Galactin-3 binding ELISA might be a useful tool for measuring the bio-functional properties of MRPs.

4.3. Advanced MR stages

The advanced MR stages seem to dominate between 45 and 90 minutes as indicated by a sharp decline in fluorescent AGEs in this timepoint. After 60 minutes, a steady but smaller increase in CML levels occurred, which correlated with a significant increase in RAGE binding. This finding is consistent with previous studies showing that CML and CEL can bind to RAGE, triggering inflammatory responses through a mechanism involving the positively charged cavity within the V-domain of RAGE.[9,14,33,56–58] Importantly, RAGE binding was specifically positively correlated with heating time with glucose, suggesting that MRPs and AGEs, rather than heated soy protein alone, are responsible for the observed increase in RAGE binding. The binding to CD36 and Galectin-3 remained stable during this stage. The UV-vis results at 420 nm revealed a marked increase in absorbance, indicating the formation of melanoidins, a key feature of advanced MRPs. Simultaneously, we observed a high and steady increase in both browning and antioxidant activity from 90 minutes onwards, suggesting that melanoidins, which are known to possess radical scavenging and Fe^{2+} chelation properties, are late-phase MRPs.[59–63] The antioxidant activity of G-SP, as measured by DPPH assay, increased rapidly after 40 minutes of heating. However, the contribution of melanoidins to antioxidant activity is difficult to quantify due to their interaction with other antioxidants, such as polyphenols and isoflavones.[39] Nonetheless, these results confirm that melanoidins are late phase MRPs, in accordance with literature.[48,59,61,63]

4.4. Immune response

In addition to studying MRP binding to AGE receptors, we investigated their ability to trigger an immune response. Previous studies have suggested that the interaction between RAGE and AGEs plays a role in modulating immune responses.[27,64,65] Our results confirm that G-SP, heated for

90 minutes, can trigger an immune response in primary monocytes, as evidenced by significant upregulation of IL-1β, IL-8, and TNF-α. These findings suggest that advanced MRPs, possibly involving RAGE, are responsible for this inflammatory response. Indeed, the RAGE antagonist FPS-ZM1 reduced IL-1β and IL-8 expression, further supporting RAGE's involvement. Interestingly, we also observed an upregulation of the anti-inflammatory cytokine IL-10, which may be attributed to the presence of melanoidins, which are upregulated after 90 minutes of heating. While RAGE has been primarily studied in the context of endogenous AGEs and inflammatory diseases[66,67] to our knowledge, this is the first report showing a RAGE-depended activation of human macrophages *via* glycated soy proteins. Our data highlight the need to investigate how dietary AGEs, such as those from glycated soy, can contribute to intestinal inflammation, as RAGE is expressed on epithelial cells and has been implicated in diseases like inflammatory bowel disease.[65] The results of the present study suggest that the types of MRPs are important factors that can influence the binding capacity of RAGE, concurring with reports regarding AGEs formed from ovalbumin (OVA) and β-lactoglobulin.[37,68] AGE-OVA and OVA modified with pyrroline are taken up *via* scavenger receptor class A; while β-lactoglobulin modified with CML was recognized by sRAGE in an inhibition ELISA assay.[37,68] Our findings emphasize the importance of understanding how food processing affects the immunogenicity of soy-based products.

5. Conclusions

Our study provides novel insights into the time-dependent formation of Maillard reaction products (MRPs) in glycated soy proteins in relation to their impact on their structural, functional, and immunological properties. We found that early MRPs characterized by early MRPs such as fructosamine and furosine, display a high fluorescence which is associated with a notably higher binding affinity for the Galectin-3 receptor compared to MRPs formed at later stages of MR. The intermediate phase showed a sharp increase in furosine, CEL and CML formation, which correlated with a significant rise in RAGE binding capacity, while the Galectin-3 binding potential sharply decreased, coinciding with a drop in the formation of fluorescent MRPs. In the advanced MR stages, CML and furosine formation were linked to increased RAGE binding and enhanced antioxidant activity. Therefore, the assessment of the dominant stages of the Maillard Reaction (MR), based on this soy-glucose model system, could be guided by chemical measurements, including markers such as fluorescence, CML, furosine, and browning index, in combination with RAGE and Galectin-3 receptor binding ELISA readouts. It is also important to note that this approach can only be applied to models that incorporate a kinetic framework, allowing the progress of the MR to be analysed as a function of time, temperature, or other critical conditions. Lastly, we demonstrated that advanced glycation of soy proteins (90 minutes, G-SP) can lead to activation of an immune response in blood-derived monocytes, likely *via* RAGE binding, suggesting a potential mechanism for the inflammatory effects of dietary AGEs. This novel approach of correlating the formation of MRPs with functional bioactivities provides a valuable tool for better understanding of how food processing impacts soy protein's immunogenicity and its health implications. Inhibition ELISA is therefore proposed as a relevant additional read-out method to measure the amount of bioactivity of MRPs formed during the processing of soy proteins and might be extended for applications to other types of food proteins.

5.1. Future directions

The health effects of dietary AGEs, particularly their impact on the body's AGE pool, remain unclear. Our study suggests that dietary AGEs may interact with immune cells and trigger inflammation. It can have a particular meaning especially in conditions with an existing gut inflammation like Inflammatory Bowel Disease (IBD) or food allergies and intolerances. Future research should focus on the digestion of glycated soy proteins to better understand potential risks, especially given the high levels of process and glycated foods in Wester diets. This could lead to improved guidelines for processing soy and other foods to reduce glycation-related harm. Our study indicates that to minimalize the binding of MRPs to RAGE and CD36 receptor the conditions of the reaction should be directed towards the formation of early and intermediate rather than advanced MRP stages. To achieve this, our data indicate the use of shorter glycation times that result in less AGE-receptor binding which might also be reached by the use of lower temperatures during heat treatment. Less binding to AGE-receptors can thereby result in lower activation of immune responses. The physiological role of the binding of early and intermediate MRPs to Galactin-3 receptor should be further explored in *in vitro* and animal models. Finally, model systems should be set up to uncover why and how specific AGEs bind to RAGE.

Author contributions

Cresci-Anne Croes and Daniela Briceno Noriega have contributed equally to this work and share first authorship.

Data availability

The authors state that the data underlying the findings of this study are included in the article and its ESI.† Raw data supporting the study's conclusions can be obtained from the corresponding author upon reasonable request.

Conflicts of interest

There are no conflicts to declare.

Acknowledgements

We would like to thank Clio Plowman, Tessa van der Loo and Iris van der Zande for their contribution in sample preparation, experiment performance and analysis.

References

1 D. Briceno Noriega, A. Breedveld, J. Ruinemmans-Koerts, H. F. J. Savelkoul and M. Teodorowicz, The effect of soy processing on its allergenicity: discrepancy between IgE binding and basophil stimulation tests, *J. Funct. Foods*, 2023, **104**, 105477.

2 K. Nishinari, Y. Fang, T. Nagano, S. Guo and R. Wang, Soy as food ingredient: Proteins Food Processing, *Woodhead Publ.*, 2018, 149–186.

3 P. Qin, T. Wang and Y. Luo, A review on plant-based proteins from soybeans: Health benefits and soy product development, *J. Agric. Food Res.*, 2022, **7**, 100265.

4 J. H. Chen, X. Lin, C. Bu and X. Zhang, Role of advanced glycation end products in mobility and considerations in possible dietary and nutritional intervention strategies, *Nutr. Metab.*, 2018, **15**, 72.

5 Q. Zhang, Y. Wang and L. Fu, Dietary advanced glycation end-products: Perspectives linking food processing with health implications, *Compr. Rev. Food Sci. Food Saf.*, 2020, **19**, 2559–2587.

6 S. I. F. S. Martins, W. M. F. Jongen and A. J. S. van Boekel, A review of Maillard reaction in food and implications to kinetic modelling, *Trends Food Sci. Technol.*, 2001, **11**, 364–373.

7 J. N. Losso, *The Maillard reaction reconsidered: cooking and eating for health*, CRC Press, 2019.

8 M. A. J. S. Van Boekel, Kinetic aspects of the Maillard reaction: a critical review, *Mol. Nutr. Food Res.*, 2001, **45**(3), 2–9.

9 C. Y. Shen, C. H. Lu, C. H. Wu, K. J. Li, Y. M. Kuo, S. C. Hsieh and C. L. Yu, The Development of Maillard Reaction, and Advanced Glycation End Product (AGE)-Receptor for AGE (RAGE) Signalling Inhibitors as Novel Therapeutic Strategies for Patients with AGE-Related Diseases, *Molecules*, 2020, **25**(23), 5591.

10 A. Twarda-Clapa, A. Olczak, A. M. Bialkowska and M. Koziolkiewicz, Advanced Glycation End-Products (AGEs): Formation, Chemistry, Classification, Receptors, and Diseases Related to AGEs, *Cells*, 2022, **11**(8), 1312.

11 C. Helou, D. Marier, P. Jacolot, L. Abdennebi-Najar, C. Niquet-Leridon, F. J. Tessier and P. Gadonna-Widehem, Microorganisms and Maillard reaction products: a review of the literature and recent findings, *Amino Acids*, 2014, **46**, 267–277.

12 N. Aljahdali and F. Carbonero, Impact of Maillard reaction products on nutrition and health: Current knowledge and need to understand their fate in the human digestive system, *Crit. Rev. Food Sci. Nutr.*, 2019, **59**(3), 474–487.

13 Z. Q. Wang and Z. Sun, Dietary N^{ε} -(carboxymethyl) lysine affects cardiac glucose metabolism and myocardial remodelling in mice, *World J. Diabetes*, 2022, **13**(11), 972–985.

14 W. Zhong-Qun, Y. Hai-Peng and S. Zhen, N^{ε} -(carboxymethyl) lysine promotes lipid uptake of macrophage via cluster of differentiation 36 and receptor for advanced glycation end products, *World J. Diabetes*, 2023, **14**(3), 222–233.

15 Q. Zhang, J. M. Ames, R. D. Smith, J. W. Baynes and T. O. Metz, A perspective on the maillard reaction and the analysis of protein glycation by mass spectrometry: probing the pathogenesis of chronic disease, *J. Proteome Res.*, 2009, **8**(2), 754–769.

16 C. Delgado-Andrade, Maillard reaction products: some considerations on their health effects, *Clin. Chem. Lab. Med.*, 2014, **52**(1), 53–60.

17 C. G. Schalkwijk, L. R. Micali and K. Wouters, Advanced glycation end-products in diabetes-related macrovascular complications: focus on methylglyoxal, *Trends Endocrinol. Metab.*, 2023, **34**, 49–60.

18 Z. Wang, J. Yan, L. Li, N. Liu, Y. Liang, W. Yuan and X. Chen, Effects of N^{ε}-carboxymethyl-Lysine on ERS-mediated apoptosis in diabetic atherosclerosis, *Int. J. Cardiol.*, 2014, **172**, e478–e483.

19 J. M. Silvan, J. van de Lagemaat, A. Olano and M. D. del Castillo, Analysis and biological properties of amino acid derivates formed by Maillard reaction in foods, *J. Pharm. Biomed. Anal.*, 2006, **41**, 1543–1551.

20 J. Uribarri, W. Cai, M. Peppa, S. Goodman, L. Ferrucci, G. Striker and H. Vlassara, Circulating glycotoxins and dietary advanced glycation end-products: two links to inflammatory response, oxidative stress, and aging, *J. Gerontol. A Biol. Sci. Med. Sci.*, 2007, **62**(4), 427–433.

21 E. N. C. Mills, *et al.*, Impact of food processing on the structural and allergenic properties of food allergens, *Mol. Nutr. Food Res.*, 2009, **53**(8), 963–969.

22 D. Briceno Noriega, H. E. Zenker, C. A. Croes, A. Ewaz, J. Ruinemans-Koerts, H. F. J. Savelkoul, *et al.*, Receptor Mediated Effects of Advanced Glycation End Products (AGEs) on Innate and Adaptative Immunity: Relevance for Food Allergy, *Nutrients*, 2022, **14**(2), 371.

23 H. Jahan and M. I. Choudhary, Gliclazide alters macrophages polarization state in diabetic atherosclerosis in vitro via blocking AGE-RAGE/TRL4-reactive oxygen species activated NF-kß nexus, *Eur. J. Pharmacol.*, 2021, **894**, 173874.

24 J. Chen, H. Peng, C. Chen, Y. Wang, T. Sang, Z. Cai, *et al.*, NAG-1/GDF15 inhibits diabetic nephropathy via inhibiting AGE/RAGE-mediated inflammation signaling pathways in C57BL/6 mice and HK-2 cells, *Life Sci.*, 2022, **311**, 121142.

25 A. M. A. Linkens, S. J. M. P. Eussen, A. J. H. M. Houben, A. Mari, P. C. Dagnelie, C. D. A. Stehouwer and C. G. Schalkwijk, Habitual intake of advanced glycation endproducts is not associated with worse insulin sensitivity, worse beta cell function, or presence of prediabetes or type 2 diabetes: The Maastricht Study, *Clin. Nutr.*, 2023, **42**(8), 1491–1500.

26 K. Maasen, S. J. P. M. Eussen, J. L. J. M. Scheijen, C. J. H. van der Kallen, P. C. Dagnelie, A. Opperhuizen, C. D. A. Stehouwer, M. M. J. van Greevenbroek and C. G. Schalkwijk, Higher habitual intake of dietary dicarbonyls is associated with higher corresponding plasma dicarbonyl concentrations and skin autofluorescence: the Maastricht Study, *Am. J. Clin. Nutr.*, 2022, **115**(1), 34–44.

27 T. Hilmenyuk, I. Bellinghausen, B. Heydenreich, A. Ichmann, M. Toda, S. Grabbe, *et al.*, Effects of glycation of the model food allergen ovalbumin on antigen uptake and presentation by human dendritic cells, *Immunology*, 2010, **129**(3), 437–445.

28 Y. Shi, M. Wang, Y. Ding, J. Chen, B. Niu and Q. Chen, Effects of Maillard reaction on structural modification and potential allergenicity of peanut 7S globulin (Ara h 1), *J. Sci. Food Agric.*, 2020, **100**(15), 5617–5626.

29 T. Kocadagli and V. Gokmen, Multiresponse kinetic modelling of Maillard reaaction and caramelization in a heated glucose/wheat flour system, *Food Chem.*, 2006, **15**(211), 892–902.

30 Y. Deng, C. Govers, S. Bastiaan-Net, N. van der Hulst, K. Hettinga and H. J. Wichers, Hydrophobicity and aggregation, but not glycation, are key determinants for uptake of thermally processed β-lactoglobulin by THP-1 macrophages, *Food Res. Int.*, 2019, **120**, 102–113.

31 L. L'Hocine, J. I. Boye and Y. Arcand, Composition and functional properties of soy protein isolates prepared using alternative defatting and extraction procedures, *J. Food Sci.*, 2006, **71**(3), 137–145.

32 P. M. Nielsen, D. Petersen and C. Dambmann, Improved Method for Determining Food Protein Degree of Hydrolysis, *J. Food Sci.*, 2001, **66**(5), 642–646.

33 H. E. Zenker, M. Teodorowicz, A. Ewaz, J. van Neerven, H. F. J. Savelkoul, N. W. De Jong, H. J. Wichers and K. A. Hettinga, Binding of cml-modified as well as heat-glycated β-lactoglobulin to receptors for AGEs is determined by charge and hydrophobicity, *Int. J. Mol.*, 2020, **21**(12), 4567.

34 M. P. Buera, J. Chirife and S. L. Resnik, Nonezymatic Nonoxidative Browing in Hydrolyzed Shelf-stable Concentrated Cheese Whey, *Food Sci.*, 1990, **55**, 697–700.

35 S. B. Matiacevich and M. P. Buera, A critical evaluation of fluorescene as a potential for the Maillard reaction, *Food Chem.*, 2006, **95**, 423–430.

36 F. L. Gu, J. M. Kim, S. Abbas, X. M. Zhang, S. Q. Xia and Z. X. Chen, Structure and antioxidant activity of high molecular weight Maillard reaction products from casein-glucose, *Food Chem.*, 2010, **120**(2), 505–511.

37 J. J. E. Janssen, B. Lagerwaard, M. Porbahaie, A. G. Nieuwenhuizen, H. F. J. Savelkoul, R. J. J. Van Neerven, *et al.*, Extra-cellular flux analyses reveal differences in mitochondrial PBMC metabolism between high-fit and low-fit females, *Am. J. Physiol. Endocrinol. Metab.*, 2022, **322**, e141–e153.

38 N. Martinez-Saez, B. Fernandez-Gomez, W. Cai, J. Urribari and M. D. Del Castillo, In vitro formation of Maillard reaction products during simulated digestion of meal-resembling system, *Food Res. Int.*, 2019, **118**, 72–80.

39 S. Yang, W. Fan and Y. Xu, Melanoidins present in traditional fermented foods and beverages, *Compr. Rev. Food Sci. Food Saf.*, 2022, **21**, 4164–4188.

40 Z. Zhang, X. M. Li, H. Xiao, A. Nowak-Wegrzyn and P. Zhou, Insight into the allergenicity of shrimp tropomyosin glycated by functional oligosaccharides containing advanced glycation end products, *Food Chem.*, 2020, 125348.

41 E. H. Anjadouz, V. Desseaux, *et al.*, Effects of temperture and pH on the kinetics of caramelisation, protein cross-linking and Maillard reactions in aqueous model systems, *Food Chem.*, 2008, **107**(3), 1244–1252.

42 S. Chawla, R. Chandler, *et al.*, Antioxidant properties of Maillard reaction products obtained by gamma-irradiation of whey proteins, *Food Chem.*, 2009, **116**(1), 122–128.

43 M. Yu, S. He, M. Tang, Z. Zhang, Y. Zhu and H. Sun, Antioxidant activity and sensory characteristics of maillard reaction products derived from different peptide fractions of soybean meal hydrolysate, *Food Chem.*, 2018, **243**, 249–257.

44 A. Schmitt, J. Schmitt, *et al.*, Characterization of advanced glyation end products for biochemical studies: side chain modifications and fluorescence characteristics, *Anal. Biochem.*, 2005, **338**(2), 201–215.

45 L. Li, Y. Zhuang, X. Zou, M. Chen, B. Cui, Y. Jiao and Y. Cheng, Advanced Glycation End Products: A Comprehensive Review of Their Detection and Occurrence in Food, *Foods*, 2023, **12**(11), 2103.

46 D. Li, X. Na, H. Wang, Y. Xie, S. Cong, Y. Song, X. Xu, B. W. Zhu and M. Tan, Fluoresencet Carbon Dots Derived from Maillard Reaction Products: Their Properties, Biodistribution, Cytotoxicity and Antioxidant Activity, *J. Agric. Food Chem.*, 2018, **66**(6), 1569–1575.

47 A. Machowska, J. Sun, A. R. Qureshi, N. Isoyama, P. Leurs, B. Anderstam, *et al.*, Plasma pentosidine and its association with mortality in patients with chronic kidney disease, *PLoS One*, 2016, **11**(10), 0163826.

48 X. Yu, M. Zhao, J. Hu, S. Zeng and X. Bai, Correspondence analysis of antioxidant activity and UV-Vis absorbane of Maillaird reaction products as related to reactants, *Food Sci. Technol.*, 2012, **46**(1), 1–9.

49 J. S. Kim and Y. S. Lee, Antioxidant activity of Maillard reaction products derived from aqueous glucose/glycine, diglycine, and tryglycine model systems as a fucntion of heating time, *Food Chem.*, 2009, **116**(1), 227–232.

50 H. Jing and D. D. Kitts, Comparison of the antioxidantive and cytotoxic propertities of glucose-lysine and fructose-lysine Maillard reaction products, *Food Res. Int.*, 2000, **33**, 509–516.

51 K. Chen, J. Zhao, X. Shi, Q. Abdul and Z. Jiang, Characterization and Antioxidants Activity of Products derived from Xylose-Bovine Casein Hydrolysate Maillard Reaction: Impact of reaction time, *Foods*, 2019, **9**(8), 242.

52 A. Tramarin, M. Naldi, G. Degani, *et al.*, Unveiling the molecular mechanisms underpinning biorecognition of early-glycated human serum albumin and receptor for advanced glycation end products, *Anal. Bioanal. Chem.*, 2020, **412**, 4245–4259.

53 C. A. C. C. Croes, M. Chrysanthou, T. Hoppenbrouwers, H. Wichers, J. Kejier, H. F. J. Savelkoul and M. Teodorowicz, Diabetic Glycation of Human Serum Albumin Affects its Immunogenicity, *Biomolecules*, 2024, **14**(12), 1492.

54 M. Teodorowicz, H. E. Zenker, A. Ewaz, T. Tsallis, A. Mauser, S. Gensberger-Reigl, N. W. de Jong, K. A. Hettinga, H. J. Wichers, R. J. J. van Neerven and H. F. J. Savelkoul, Enhanced Uptake of Processed Bovine β-Lactoglobulin by Antigen Presenting Cells: Identification of Receptors and Implications for Allergenicity, *Mol. Nutr. Food Res.*, 2021, **65**(8), e2000834.

55 H. Li and S. J. Yu, Review of pentosidine and pyrraline in food and chemical models: formation, potential risks and determination, *J. Sci. Food Agric.*, 2018, **98**(9), 3225–3233.

56 S. J. Loomis, Y. Chen, D. B. Sacks, E. S. Christenson, R. H. Christenson, C. M. Rebholz and E. Selvin, Cross-sectional analysis of AGE-CML, sRAGE and esRAGE with diabetes and cardiometabolic risk factors in a community-based cohort, *Clin. Chem.*, 2017, **63**(5), 980–989.

57 G. A. Mueller, S. J. Maleki, K. Johnson, B. K. Hurlburt, H. Cheng, S. Ruan, *et al.*, Identification of Maillard reaction products on peanut allergens that influence binding to the receptor for advanced glycation end products, *Allergy*, 2013, **68**(12), 1546–1554.

58 T. Kislinger, C. Fu, B. Huber, W. Qu, A. Taguchi, S. Yan, *et al.*, Nε-(carboxymethyl) lysine adducts of proteins are ligands for receptor for advanced for glycation end products that activate cell signaling pathways and modulate gene expression, *J. Biol. Chem.*, 1999, **274**, 31740–31749.

59 F. J. Morales, V. Somoza and V. Fogliano, Physiological Relevance of Dietary Melanoidins, *Amino Acids*, 2012, **42**(4), 1097–1109.

60 M. J. Kim, H. S. Kwak and S. S. Kim, Effects of salinity on bacterial communities, Maillard reactions, isoflavone antioxidation and antiproliferation in Korean fermented soybean paste (doenjang), *Food Chem.*, 2018, **245**, 402–409.

61 Y. Li, J. Ouyyang, W. Su, X. Zheng and L. Jiang, Protein biological changes and antioxidant capacity of traditional fermented douchi, *China Brew.*, 2013, **33**(11), 2024.

62 C. H. Guo, L. Lin, Z. H. Chen, Z. H. Lu, L. P. Sun and J. Yu, Extraction, spectral properties and bioactive functions of melanoidins from black soy sauce, *Food Sci.*, 2012, **33**(11), 89–93.

63 S. Pastoriza and J. A. Rurian-Henares, Contribution of melanoidins to the antioxidant capacity of the Spanish diet, *Food Chem.*, 2014, **164**, 438–445.

64 J. R. Erusalimsky, The use of the soluble receptor for advanced glycation-end products (sRAGE) as a potential biomarker of disease and adverse outcomes, *Redox Biol.*, 2021, **42**, 101958.

65 M. Body-Malapel, M. Djouina, C. Waxin, A. Langlois, C. Gower-Rousseau, P. Zerbib, *et al.*, The RAGE signaling pathway is involved in intestinal inflammation and represents a promising therapeutic target for Inflammatory Bowel Disease, *Mucosal Immunol.*, 2019, **12**(2), 468–478.

66 N. L. Reynaert, P. Gopal, E. P. A. Rutten, E. F. M. Wouters and C. G. Schalkwijk, Advanced glycation end products and their receptor in age-related, non-communicable chronic inflammatory diseases; Overview of clinical evidence and potential contributions to disease, *Int. J. Biochem. Cell Biol.*, 2016, **81**, 403–418.

67 N. Kumari, D. Bandyopadhyay, V. Kumar, D. B. Venkatesh, S. Prasad, S. Prakash, P. R. Krishnaswamy, P. Balaram and N. Bhat, Glycation of albumin and its implication in Diabetes: A comprehensive analysis using mass spectrometry, *Clin. Chim. Acta*, 2021, **520**, 108–117.

68 m. Heilmann, A. Wellner, G. Gadermaier, A. Ilchmann, P. Briza, M. Krause, *et al.*, Ovalbumin Modified with Pyraline, a Maillard Reaction Product, shows Enhanced T-cell Immunogenicity, *Immunology*, 2014, **289**(11), 7919–7928.

